Impact of the dark path on quantum dot single photon emitters in small cavities

Kenji Kamide,[1,*] Satoshi Iwamoto,[1,2] and Yasuhiko Arakawa[1,2]
[1]Institute of Industrial Science, University of Tokyo, Tokyo 153-8505, Japan
[2]Institute for Nano Quantum Information Electronics (NanoQuine), University of Tokyo, Tokyo 153-8505, Japan
(Received 13 May 2014; published 2 October 2014)

Incoherent pumping in quantum dots can create a biexciton state through two paths: via the formation of bright or dark exciton states. The latter, dark-pumping path is shown to enhance the probability of two-photon simultaneous emission and hence increase $g^{(2)}(0)$ by a factor $\propto 1/\gamma_S$, due to the slow spin relaxation rate γ_S in quantum dots. The existence of the dark path is shown to impose a limitation on the single photon emission process, especially in nanocavities which exhibit a large exciton-cavity coupling and a Purcell enhancement for fast quantum telecommunications.

DOI: 10.1103/PhysRevLett.113.143604 PACS numbers: 42.50.Pq, 71.35.-y, 78.67.Hc

Introduction.—A high quality single photon (SP) source is essential for the realization of secure telecommunications based on the principles of quantum mechanics, such as quantum key distribution (QKD) [1]. Semiconductor quantum dots (QDs) are promising candidates for solid-state SP emitters because of their well-defined atomlike quantized states [2–6], and a high controllability of their emission wavelength [7]. Interactions between QD excitons and photons are also controllable by embedding QDs in optical nanocavities [8] in which cavity quantum electrodynamics (cavity QED) effects have been observed [9,10].

The quality of a SP emitter is quantified by measuring the conditional probability to observe photons at a delay time τ after a photon counting event, $g^{(2)}(\tau)$ [11,12]. The value of $g^{(2)}(\tau)$ at zero time delay, $g^{(2)}(0)$, should be as close as possible to zero to obtain pure SP emission. This is equivalent to minimizing the probability of finding multiple-photon simultaneous emissions. For application in QKD, a high emission rate is also desired, which can be attained if QDs are combined with optical microcavities [13–17].

In this Letter, we investigate incoherent pumping (by above-band-gap laser excitation or current injection) in a QD SP emitter to find a "dark path"; a pumping path from ground to biexciton states via a dark exciton state can strongly increase $g^{(2)}(0)$, thus imposing a limit on the available SP purity, especially in small cavities with a small mode volume, V_{mode}, and a large exciton-cavity coupling, $g \propto 1/\sqrt{V_{\mathrm{mode}}}$. In the following, we define $\hbar = 1$ for simplicity.

Impact of the dark path in QD SP emitters without cavities.—In order to see how the dark path increases the multiple-photon-emission probability, we first study a simple phenomenological model for a QD SP emitter without cavity coupling. Here, an undoped QD is pumped incoherently and continuously under a charge-neutral condition. The QD states relevant to our study are restricted to the neutral states with up to two electron-hole pairs, as shown in Fig. 1(a). Excited carriers injected at high energy levels become trapped in the lowest QD level after fast relaxation from a continuum above the band gap and excited trapped states (which are truncated in our model). The whole process of injection and relaxation of the carriers (electron-hole pairs) to the lowest QD level is described by pumping rate P. Depending on the spins of carriers, the bright and dark excitons (BX and DX) are randomly generated from the initial empty state (G) with the same rate P. Successive creations of two electron-hole pairs further excite the system to the biexciton state, XX. The SP emission process is mainly governed by the exciton recombination (with the rate γ_X), and the two-photon emission process by the biexciton-exciton cascaded recombinations (their energy difference is the biexciton binding energy $-\chi = E_{XX} - E_X$). In QDs, spin relaxation processes between BX and DX (the rate γ_S) are usually slow [18,19] and often neglected; however, they must be considered carefully to evaluate $g^{(2)}(0)$, as shown below.

The rate equations for the populations at each QD level are $\dot{\rho}_G = -2P\rho_G + \gamma_X\rho_{BX}$, $\dot{\rho}_{DX} = -(\gamma_S + P)\rho_{DX} + P\rho_G + \gamma_S\rho_{BX}$, $\dot{\rho}_{BX} = -(\gamma_X + \gamma_S + P)\rho_{BX} + P\rho_G + \gamma_{XX}\rho_{XX} + \gamma_S\rho_{DX}$, and $\dot{\rho}_{XX} = -\gamma_{XX}\rho_{XX} + P\rho_{DX} + P\rho_{BX}$ [20], for which the steady state satisfies

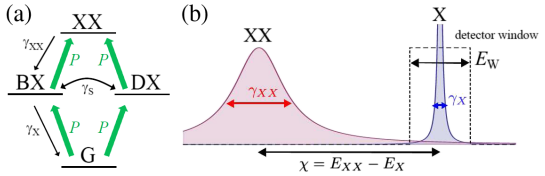

FIG. 1 (color online). (a) Illustration of the rate equation model for a neutral QD with ground, bright and dark exciton, and biexciton states (G, BX, DX, and XX). (b) Spectral profiles of the biexciton and exciton emissions. A spectral filter with a detection window E_W ($> \gamma_X$) is also shown.

$$\rho_{XX} = \left(1 + \frac{\gamma_X}{4\gamma_S}\right)\frac{4P^2}{\gamma_X\gamma_{XX}} + \mathcal{O}(P^3), \quad (1)$$

$$\rho_{BX} = 2P/\gamma_X + \mathcal{O}(P^2), \quad (2)$$

$$\rho_{DX} = (\gamma_S^{-1} + 2\gamma_X^{-1})P + \mathcal{O}(P^2), \quad (3)$$

in the linear regime at weak pumping. From this result, the normalized second order correlation function is given by $g^{(2)}(0) = f_{XX} \times (\gamma_X\gamma_{XX}\rho_{XX})/(\gamma_X\rho_{BX})^2$ [21]. Here, $f_{XX} \equiv \frac{1}{\pi}\int_{E_X-E_W/2}^{E_X+E_W/2}((\gamma_{XX})/\gamma_{XX}^2 + (\omega - E_{XX})^2)d\omega$ is the probability of finding a photon emitted from XX within the detector spectral window [Fig. 1(b)]. Under the assumptions that $\chi \gg E_W$, $\chi \gg \gamma_{XX}$, and $E_W > \gamma_X$, we have $f_{XX} \sim \pi^{-1}(\gamma_{XX}/\chi)^2(E_W/\gamma_{XX})$ and, hence, in the linear regime

$$g^{(2)}(0) = \frac{1}{\pi}\left(\frac{\gamma_{XX}}{\chi}\right)\left(\frac{E_W}{\chi}\right)\left(1 + \frac{\gamma_X}{4\gamma_S}\right). \quad (4)$$

The factor $(1/\pi)(\gamma_{XX}/\chi)(E_W/\chi)$ can be naturally understood since a small E_W and a large χ [22,23] would act to reduce the probability of counting unwanted photons from the XX emission. On the other hand, the extra factor, $(1 + (\gamma_X/4\gamma_S))$, which becomes large [24] when the spin relaxation is very slow ($\gamma_S \ll \gamma_X$), needs a deeper explanation.

The enhancement of $g^{(2)}(0)$ by this factor occurs due to an unwanted excitation of state XX through a dark path—a path via the excitation of DX. This can be verified by testing another model without the dark path: We find that $g^{(2)}(0) = \pi^{-1}\gamma_{XX}E_W\chi^{-2}$ if the DX state and the "dark" pumping path are not present [this result is also obtained when $\gamma_S \gg \gamma_X$ in Eq. (4)]. The above scenario can also be verified from the steady state population in Eq. (2) and Eq. (3): The ratio ρ_{DX}/ρ_{BX} diverges as $\gamma_S/\gamma_X \to 0$ so that the production rate of ρ_{XX} is largely enhanced when the dark pumping path is present.

Following the simple discussion above, we find that the dark path can act as a bottleneck when trying to purify the SP generation in QDs since the spin relaxation process is usually slower (typically 1–10 ns time scale) than the other processes [18,19]. The effect found in neutral QDs survives even if charged states temporarily exist, as long as the charge relaxation is fast [25]. The strong impact of a dark pumping path on $g^{(2)}(0)$ has been shown for many two-level atoms or many QDs by Temnov *et al.* [26], where the connection with cooperative spontaneous emission and superradiance is also discussed. Even though the system considered here is a single emitter, similar physics does exist and can reduce the quality of a SP emitter.

Impact of the dark path on high-speed SP emitters with cavities.—We next shift our discussion to how the use of an optical microcavity [13,14,16] affects the SP purity. The realization of high quality SP sources in microcavities has become an important issue [17]. Hence, it is important to understand what effects such a dark path may have on QDs in microcavities. From the result obtained in the previous section, [Eq. (4)], one may guess that the Purcell enhancement in γ_X would result in the increase in $g^{(2)}(0)$, and hence that the dark path pumping might be more troublesome than in a system without a cavity. However, the discussion without cavity cannot be applied directly to this case. Here we investigate the effect of a microcavity within the cavity QED framework with quantum master equations (QME) [12].

We consider a system that consists of carriers inside a QD and photons interacting inside a cavity. Six electronic configurations are considered: an empty state, $|G\rangle$; two bright exciton states, $|BX1\rangle = e_\uparrow^\dagger h_\downarrow^\dagger|G\rangle$ and $|BX2\rangle = e_\downarrow^\dagger h_\uparrow^\dagger|G\rangle$; two dark exciton states, $|DX1\rangle = e_\uparrow^\dagger h_\uparrow^\dagger|G\rangle$ and $|DX2\rangle = e_\downarrow^\dagger h_\downarrow^\dagger|G\rangle$; and a biexciton state, $|XX\rangle = e_\uparrow^\dagger e_\downarrow^\dagger h_\uparrow^\dagger h_\downarrow^\dagger|G\rangle$, where e_σ and h_σ ($e_\sigma^\dagger$ and $h_\sigma^\dagger$) are annihilation (creation) operators of electrons and holes with spin $\sigma = \uparrow, \downarrow$ in their respective lowest energy levels of the QD. The cavity photon number is $a^\dagger a$, where a and $a^\dagger$ are the annihilation and creation operators, respectively. Assuming the frequencies of the cavity (ω_C) and the exciton (ω_X) are tuned to resonance, $\omega_C = \omega_X \equiv \omega_0$, the Hamiltonian of the coupled QD-cavity system [27] is

$$H = \omega_0 N_{\text{tot}} - \chi|XX\rangle\langle XX| + \sum_{i=\text{BX1,BX2}} g_X a^\dagger|G\rangle\langle i| + g_{XX}a^\dagger|i\rangle\langle XX| + \text{H.c.}, \quad (5)$$

where $N_{\text{tot}} = \sum_{\sigma=\uparrow,\downarrow}(e_\sigma^\dagger e_\sigma + h_\sigma^\dagger h_\sigma)/2 + a^\dagger a$ is the total excitation number, and we put $g_X = g_{XX} \equiv g$ in the simulations for simplicity. Assuming the dynamics in the environment (pump and decay baths outside the coupled QD-cavity system) are fast and uncorrelated, the time evolution of the system density matrix is given by Markovian QME, $(d/dt)\rho = i[\rho, H] + \mathcal{L}\rho$ [12], where, for this QD-cavity system [27,28],

$$\mathcal{L}\rho = \left(\kappa\mathcal{L}_a + P\sum_{\sigma,\sigma'}\mathcal{L}_{h_{\sigma'}^\dagger e_\sigma^\dagger} + \sum_\sigma(\gamma_{sp}\mathcal{L}_{e_\sigma h_{-\sigma}} + \Gamma_{\text{ph}}\mathcal{L}_{e_\sigma^\dagger e_\sigma} + \Gamma_{\text{ph}}\mathcal{L}_{h_\sigma^\dagger h_\sigma} + \gamma_S^e\mathcal{L}_{e_\sigma^\dagger e_{-\sigma}} + \gamma_S^h\mathcal{L}_{h_\sigma^\dagger h_{-\sigma}})\right)\rho. \quad (6)$$

Using the standard notation, $\mathcal{L}_A\rho \equiv \frac{1}{2}(2A\rho A^\dagger - A^\dagger A\rho - \rho A^\dagger A)$, we consider the following processes: the spontaneous emission into the cavity mode (the couplings, g_X and g_{XX}) and free space (the rate γ_{sp}) [29], cavity loss (the rate κ), dephasing of polarizations (rate Γ_{ph}), the spin flip of electrons and holes (the rates γ_S^e and γ_S^h), and the resulting transitions between dark and bright excitons (the rate $\gamma_S = \gamma_S^e + \gamma_S^h$).

One could determine the nonequilibrium steady state, ρ_∞, by numerically performing a longtime evolution of the

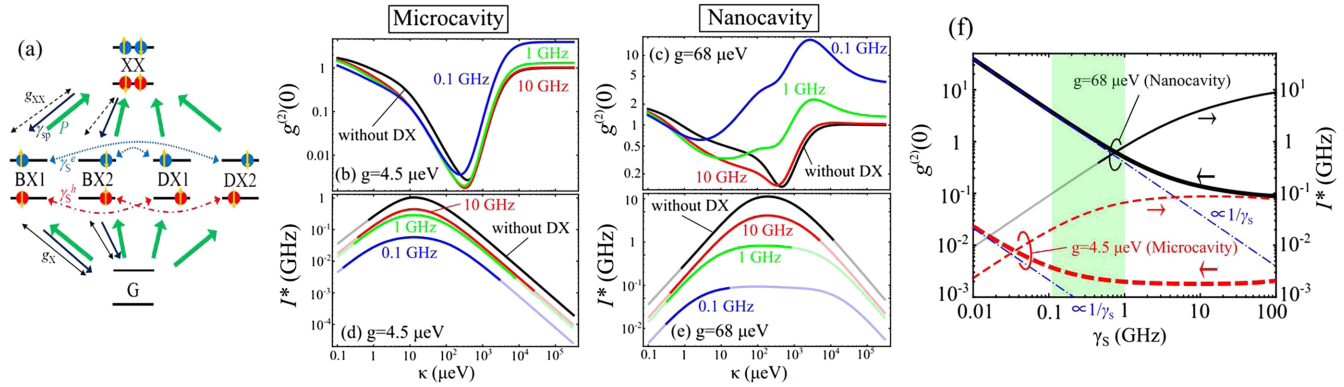

FIG. 2 (color online). (a) A neutral QD model with full consideration of carrier spins for SP emitters with cavities. The image shows the empty, bright and dark exciton, and biexciton states (G, BX1, BX2, DX1, DX2, and XX). (b),(c) $g^{(2)}(0)$ and (d),(e) a crossover photon emission rate, I^*, plotted as a function of the cavity loss κ for (b),(d) a microcavity with $V_{\text{mode}} \sim 15 \times 15 \times 1\ \mu\text{m}^3$ and $g = 4.5\ \mu\text{eV}$, and for (c),(e) a ultrasmall nanocavity with $V_{\text{mode}} \sim 1 \times 1 \times 1\ \mu\text{m}^3$ and $g = 68\ \mu\text{eV}$ [10,14]. Three spin relaxation rates, $\gamma_S = 0.1$, 1, 10 GHz, are used as indicated in the plots. (f) $g^{(2)}(0)$ (thick line) and I^* (thin line) as a function of spin relaxation rate γ_S for $g = 4.5\ \mu\text{eV}$ (red dashed line) and $g = 68\ \mu\text{eV}$ (black solid line) with $\kappa = 300\ \mu\text{eV}$. Dot-dashed lines: guides for the eye on $g^{(2)}(0) \propto 1/\gamma_S$. The green shaded area indicates a typical parameter range for InAs QDs, 0.1 GHz $< \gamma_S <$ 1 GHz. In all plots, typical parameters of InAs QDs are chosen: $\gamma_{sp} = 0.77\ \mu\text{eV} = 1/(0.85\ \text{ns})$, $\Gamma_{\text{ph}} = 15\ \mu\text{eV}$, and $\chi = 2$ meV. Pale parts of the plots in (d)–(f) are corresponding to the regime where $g^{(2)}(0) > 1$ in (b),(c) and I^* cannot be a measure of the maximum available emission rate as a quantum light source [33].

system, to obtain the photon number $\langle a^\dagger a\rangle$ and $g^{(2)}(0) = \langle a^\dagger a^\dagger a a\rangle / |\langle a^\dagger a\rangle|^2$. However, we choose an alternative analytic approach to find the photon correlation functions, which is allowed in the linear regime at small P and can be performed by a perturbation method [30–32]. This analytic approach allows clear insight into the physics and greatly reduces the calculation time to obtain the properties of photons as a function of numbers of parameters (κ, P, γ_{sp}, Γ_{ph}, γ_S, χ) [33].

Figures 2(b) and 2(c) and 2(d) and 2(e) show the $g^{(2)}(0)$ and the crossover photon emission rate $I^* \equiv \kappa\langle a^\dagger a\rangle$ at a crossover pump rate between the linear and nonlinear regime, P^* [33], as a function of κ for a microcavity and a nanocavity, respectively. Here we define $P^* \equiv 0.5 \times \min(|A_1/A_2|, |B_1/B_2|)$ using perturbation expansions, $\langle a^\dagger a\rangle = A_1 P + A_2 P^2 + \mathcal{O}(P^3)$ and $\langle |\text{BX1}\rangle\langle\text{BX1}|\rangle = B_1 P + B_2 P^2 + \mathcal{O}(P^3)$ (the second order corrections amount to 50 percent of the first order ones at P^*). Since the SP purity degrades at $P > P^*$ when $g^{(2)}(0) < 1$ in the weak pump limit, I^* indicates the maximum available photon emission rate with $g^{(2)}(0)$ being kept small. Figures 2(b) and 2(d) show the results for a microcavity (as in [14]) with $V_{\text{mode}} \sim 15 \times 15 \times 1\ \mu\text{m}^3$ and $g = 4.5\ \mu\text{eV}$. Figures 2(c) and 2(e) show the results for an ultrasmall nanocavity structure (a photonic crystal nanocavity as in [10]), with $V_{\text{mode}} \sim 1 \times 1 \times 1\ \mu\text{m}^3$ and $g = 68\ \mu\text{eV}$. In each plot, three spin relaxation rates, $\gamma_S = 0.1$, 1, and 10 GHz, are examined. Here, the spontaneous emission rate $\gamma_{sp} = 0.77\ \mu\text{eV} = 1/(0.85\ \text{ns})$, dephasing rate $\Gamma_{\text{ph}} = 15\ \mu\text{eV}$, and the biexciton binding energy $\chi = 2$ meV are typical values for indium arsenide (InAs) QDs.

Interestingly, the figures exhibit an optimal $\kappa \equiv \kappa_{\text{opt},1}$ minimizing $g^{(2)}(0)$ [$\kappa_{\text{opt},1} \sim 300\ \mu\text{eV}$ for $\gamma_S = 10$ GHz in Figs. 2(b) and 2(c)]. This is in remarkable contrast to ordinary cavity QED with a two-level atom [31,32], in which $g^{(2)}(0)$ monotonically decreases with increasing κ. Thus, we understand that the existence of $\kappa_{\text{opt},1}$ is due to the existence of the biexciton (multiple exciton) state. The value of the optimal loss, $g < \kappa_{\text{opt},1} < \chi$, is explained as follows: (i) For good cavities with $\kappa \ll g$, photons accumulate in the cavity resulting in the non-negligible multiple-photon probability resulting in a decreasing $g^{(2)}(0)$ with increasing κ [28]; (ii) in the weak coupling regime $\kappa \gg g$, the rate of exciton and biexciton transitions into the cavity mode ($W_X = 2g^2/\kappa$, $W_{XX} = 2g^2\kappa/(\kappa^2 + \chi^2)$ becomes the same for $\kappa \gg \chi$ and the cascaded two-photon emission is relatively enhanced, resulting in the increase in $g^{(2)}(0)$ with κ [34]. The figures also show an optimal loss $\kappa_{\text{opt},2} = \mathcal{O}(g)$, maximizing I^*, which is not surprising since I^* is determined by the small output rate, κ, and the small emission rate, W_X, for $\kappa \ll g$ and $\kappa \gg g$, respectively.

An important finding is that for the larger microcavity in Fig. 2(b), the values of $g^{(2)}(0)$ at the minima do not change much for the whole range, 0.1 GHz $< \gamma_S <$ 10 GHz. On the other hand, for the smaller nanocavity in Fig. 2(c), one finds a large enhancement in $g^{(2)}(0)$ for the slow spin relaxation, $\gamma_S <$ 1 GHz. QDs in a nanocavity with $\gamma_S =$ 0.1 GHz cannot be considered as a SP emitter since $g^{(2)}(0)$ never falls below 0.5 (unless some means were taken as mentioned below). Therefore, the impact of the dark path is stronger in smaller cavities, which agrees with the simple intuitive guess made at the beginning of this section. For comparison, we also show results for the QD model

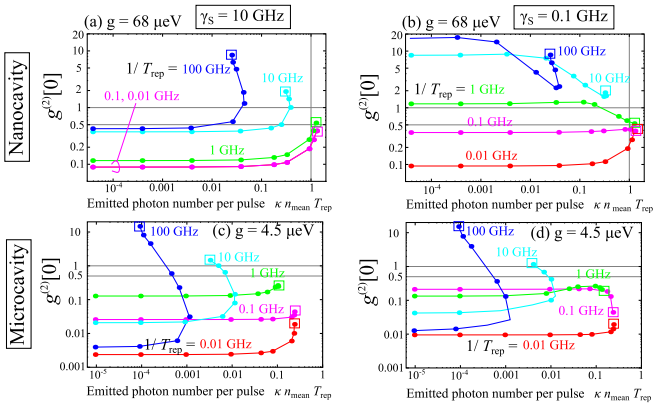

FIG. 3 (color online). $g^{(2)}[0]$ values (averaged within a pulse [35]) are plotted as a function of mean number of emitted photons per pulse, $\kappa n_{\mathrm{mean}} T_{\mathrm{rep}}$, for ultrashort-pulse excitations of various repetition rates, $1/T_{\mathrm{rep}} = 100$, 10, 1, 0.1, 0.01 GHz, for a nanocavity, $g = 68$ μeV, with (a) $\gamma_S = 10$ GHz and (b) 0.1 GHz, and for a microcavity, g = 4.5 μeV, with (c) $\gamma_S = 10$ GHz and (d) 0.1 GHz. Other parameters $(\kappa, \gamma_{sp}, \Gamma_{\mathrm{ph}}, \chi) = (300, 0.77, 15, 2000)$ μeV are the same as Fig. 2(f). End points in boxes correspond to saturation points where each pulse creates biexciton states perfectly [35]. Solid lines are a guide for the eyes.

without the dark states and dark paths [34] [solid black curves in Figs. 2(b)–2(e)], where the clear increase in $g^{(2)}(0)$ at $\kappa = \kappa_{\mathrm{opt},1}$ is found for small γ_S in Fig. 2(c). A reduction of I^* due to the dark path, claimed by Strauf *et al.* [14], is also found in Figs. 2(d) and 2(e), and the reduction is much more pronounced for the nanocavity in Fig. 2(e). (The nanocavity exhibits a more than tenfold decrease at $\kappa = \kappa_{\mathrm{opt},2}$ for $\gamma_S = 1$ GHz.)

Figure 2(f) shows the γ_S dependencies of $g^{(2)}(0)$ and I^* for a cavity loss $\kappa = 300$ μeV (chosen around $\kappa = \kappa_{\mathrm{opt},1}$). For both cavities, $g^{(2)}(0)$ is proportional to $1/\gamma_S$ at small γ_S due to the enhanced dark path effect. The $1/\gamma_S$ dependency (the degradation of SP purity) originates from the same physics explained above and in Eq. (4). We should note that the dependency is found in the typical parameter regime [0.1 GHz $< \gamma_S <$ 1 GHz: the shaded region in Fig. 2(f)] only for nanocavities, not for microcavities.

The degradation of SP purity by the dark pumping path is also found when the pump excitations are short-pulse sequences. In Fig. 3, we show the second order correlation function at zero time delay $g^{(2)}[0]$ (averaged within a pulse [35]) as a function of mean number of emitted photons per pulse, $\kappa n_{\mathrm{mean}} T_{\mathrm{rep}}$ with $n_{\mathrm{mean}} \equiv T_{\mathrm{rep}}^{-1} \int_0^{T_{\mathrm{rep}}} \langle a^\dagger(t) a(t) \rangle dt$, for various pulse repetition rates ($1/T_{\mathrm{rep}} = 0.1$–100 GHz) and for different cavities ($g = 68$, 4.5 μeV). If the pulse repetition is faster than spin relaxation ($1/T_{\mathrm{rep}} > \gamma_S$), DX states created by a given pulse cannot relax to BX states before the next pulse arrives, and therefore XX is likely to be created by the next pulse, resulting in the increase of $g^{(2)}[0]$. Similar to the cw pumping case, the degradation effect is rather weak for the microcavity [$g = 4.5$ μeV: Figs. 3(c) and 3(d)], albeit, in this case the emission rate cannot reach one photon per pulse due to a small fraction of the cavity emission $W_X/(\gamma_{sp} + W_X)$. High-rate SP generation (with high $1/T_{\mathrm{rep}}$) is especially limited by the slow spin relaxation of QDs for nanocavities, as shown in Figs. 3(a) and 3(b) [although SP emission with $g^{(2)}[0] = 0.32$ at 1 GHz repetition is possible with an unrealistically high spin flip rate of 10 GHz, as shown in Fig. 3(a)].

Summary.—The strong impact of the dark path—a pumping path via dark exciton states to biexciton states—on the quality of SP emitters has been shown to exist in QD systems. The increase in $g^{(2)}(0)$, observed irrespective of whether the pumping is cw or short-pulse sequences, indicates the dark path can reduce the quality of QD SP emitters, especially those situated in small cavities like nanocavities.

Finally, we mention several ways to reduce the impact of the dark path for an application purpose: (i) The use of a charged exciton state $X_\pm$ where there is no dark path [14]; (ii) the use of resonant and coherent laser excitation [36–40], which automatically selects to create bright states only; (iii) enhancement of the spin relaxation rate [18] to suppress the unwanted multiple photon emission; (iv) selection of QDs with a large biexciton binding energy [22] in order to limit the spectral overlap of cascaded photons; and (v) the use of a spectral filter can partly reduce the unwanted output from XX emission if the filter bandwidth were optimally selected [41].

We thank Y. Ota, M. Holmes, S. Kako, and T. Miyazawa for the useful comments and discussions. This work is supported by the Project for Developing Innovation Systems of MEXT, Japan.

*kamide@iis.u-tokyo.ac.jp

[1] C. H. Bennett and G. Brassard, in *Proceedings of the IEEE International Conference on Computers, Systems and Signal Processing, Bangalore, India, 1984* (IEEE, New York, 1984), p. 175; IBM Technical Disclosure Bulletin **28**, 3153 (1985).
[2] E. Waks, K. Inoue, C. Santori, D. Fattal, J. Vuckovic, G. S. Solomon, and Y. Yamamoto, Nature (London) **420**, 762 (2002).
[3] C. Santori, M. Pelton, G. Solomon, Y. Dale, and Y. Yamamoto, Phys. Rev. Lett. **86**, 1502 (2001).
[4] K. Takemoto *et al.*, Appl. Phys. Express **3**, 092802 (2010).
[5] S. Kako, C. Santori, K. Hoshino, S. Götzinger, Y. Yamamoto, and Y. Arakawa, Nat. Mater. **5**, 887 (2006).
[6] M. J. Holmes, K. Choi, S. Kako, M. Arita, and Y. Arakawa, Nano Lett. **14**, 982 (2014).
[7] T. Nakaoka, Y. Tamura, T. Miyazawa, K. Watanabe, Y. Ota, S. Iwamoto, and Y. Arakawa, Jpn. J. Appl. Phys. **51**, 02BJ05 (2012).
[8] E. Yablonovitch, Phys. Rev. Lett. **58**, 2059 (1987).

[9] T. Yoshie, A. Scherer, J. Hendrickson, G. Khitrova, H. M. Gibbs, G. Rupper, C. Ell, O. B. Shchekin, and D. G. Deppe, Nature (London) **432**, 200 (2004).

[10] M. Nomura, N. Kumagai, S. Iwamoto, Y. Ota, and Y. Arakawa, Nat. Phys. **6**, 279 (2010).

[11] R. Hanbury-Brown and R. Q. Twiss, Nature (London) **177**, 27 (1956).

[12] H. J. Carmichael, *Statistical Methods in Quantum Optics 1: Master Equations and Fokker-Planck Equations*, 2nd ed. (Springer-Verlag, Berlin, 2003).

[13] D. Englund, D. Fattal, E. Waks, G. Solomon, B. Zhang, T. Nakaoka, Y. Arakawa, Y. Yamamoto, and J. Vučković, Phys. Rev. Lett. **95**, 013904 (2005).

[14] S. Strauf, N. G. Stoltz, M. T. Rakher, L. A. Coldren, P. M. Petroff, and D. Bouwmeester, Nat. Photonics **1**, 704 (2007).

[15] D. J. Ellis, A. J. Bennett, S. J. Dewhurst, C. A Nicoll, D. A. Ritchie, and A. J. Shields, New J. Phys. **10**, 043035 (2008).

[16] M. D. Birowosuto, H. Sumikura, S. Matsuo, H. Taniyama, P. J. van Veldhoven, R. Nötzel, and M. Notomi, Sci. Rep. **2**, 321 (2012).

[17] S. Buckley, K. Rivoire, and J. Vučković, Rep. Prog. Phys. **75**, 126503 (2012).

[18] J. M. Smith, P. Dalgarno, R. Warburton, A. Govorov, K. Karrai, B. Gerardot, and P. Petroff., Phys. Rev. Lett. **94**, 197402 (2005).

[19] M. Paillard, X. Marie, P. Renucci, T. Amand, A. Jbeli, and J. Gérard., Phys. Rev. Lett. **86**, 1634 (2001).

[20] If QD states are restricted to the neutral states, the rate equation can be derived from the diagonal part of the quantum master equation by using the electron-hole operators $e^{\dagger}_{\sigma} h^{\dagger}_{\sigma'}$ in the pump terms since the Paul exclusion principle of the carriers (as referred to in [28]) is automatically fulfilled. As long as the charge neutrality is approximately satisfied, this rate equation is valid.

[21] Following a discussion in Sec. 2.3 of [12], $g^{(2)}(0) = \langle :\hat{I}\,\hat{I}: \rangle / \langle \hat{I} \rangle^2$, where $\hat{I} \equiv \gamma_X \hat{S}^+_X \hat{S}^-_X + f_{XX}\gamma_{XX} \times \hat{S}^+_{XX}\hat{S}^-_{XX}$ is the operator for the total emission rate into the detector window, $\hat{S}^+_X = (\hat{S}^-_X)^\dagger \equiv |BX\rangle\langle G|$, and $\hat{S}^+_{XX} = (\hat{S}^-_{XX})^\dagger \equiv |XX\rangle\langle BX|$. In the normal ordered product, $\langle :\hat{I}\,\hat{I}: \rangle = f_{XX}\gamma_{XX}\gamma_X \langle \hat{S}^+_{XX}\hat{S}^+_X\hat{S}^-_X\hat{S}^-_{XX}\rangle$. In the denominator, the dominant linear-order term in P is $\langle \hat{I} \rangle = \gamma_X \langle \hat{S}^+_X \hat{S}^-_X \rangle$.

[22] W. Langbein, P. Borri, U. Woggon, V. Stavarache, D. Reuter, and A. D. Wieck, Phys. Rev. B **69**, 161301(R) (2004).

[23] R. Trotta, E. Zallo, E. Magerl, O. G. Schmidt, and A. Rastelli, Phys. Rev. B **88**, 155312 (2013).

[24] In an ideal case $\gamma_S = 0$, we have $\rho_{XX}/\rho^2_{BX} \approx \gamma^2_X/(2\gamma_{XX}P)$.

[25] See Sec. E of Supplemental Material at http://link.aps.org/supplemental/10.1103/PhysRevLett.113.143604 for a detailed analysis on the effect of charged states.

[26] V. V. Temnov and U. Woggon, Opt. Express **17**, 5774 (2009).

[27] M. Yamaguchi, T. Asano, K. Kojima, and S. Noda, Phys. Rev. B **80**, 155326 (2009).

[28] S. Ritter, P. Gartner, C. Gies, and F. Jahnke, Opt. Express **18**, 9909 (2010).

[29] J. Johansen, S. Stobbe, I. Nikolaev, T. Lund-Hansen, P. Kristensen, J. Hvam, W. Vos, and P. Lodahl, Phys. Rev. B **77**, 073303 (2008).

[30] G. S. Agarwal and S. Dutta Gupta, Phys. Rev. A **42**, 1737 (1990).

[31] E. del Valle, F. P. Laussy, and C. Tejedor, Phys. Rev. B **79**, 235326 (2009).

[32] P. Gartner, Phys. Rev. A **84**, 053804 (2011).

[33] See Secs. A and B of Supplemental Material [42] at http://link.aps.org/supplemental/10.1103/PhysRevLett.113.143604 for details of the derivation and calculations.

[34] See Sec. C of Supplemental Material [42] at http://link.aps.org/supplemental/10.1103/PhysRevLett.113.143604 for details of the derivation and calculations.

[35] See Sec. D of Supplemental Material [42] at http://link.aps.org/supplemental/10.1103/PhysRevLett.113.143604 for the method of evaluations for short-pulse excitations.

[36] M. Paillard, X. Marie, E. Vanelle, T. Amand, V. K. Kalevich, A. R. Kovsh, A. E. Zhukov, and V. M. Ustinov, Appl. Phys. Lett. **76**, 76 (2000).

[37] A. Muller, E. B. Flagg, P. Bianucci, X. Y. Wang, D. G. Deppe, W. Ma, J. Zhang, G. J. Salamo, M. Xiao, and C. K. Shih, Phys. Rev. Lett. **99**, 187402 (2007).

[38] A. N. Vamivakas, Y. Zhao, C.-Y. Lu, and M. Atatüre, Nat. Phys. **5**, 198 (2009).

[39] S. Ates, S. Ulrich, S. Reitzenstein, A. Löffler, A. Forchel, and P. Michler, Phys. Rev. Lett. **103**, 167402 (2009).

[40] D. Englund, A. Majumdar, A. Faraon, M. Toishi, N. Stoltz, P. Petroff, and J. Vučković, Phys. Rev. Lett. **104**, 073904 (2010).

[41] K. Kamide, S. Iwamoto, and Y. Arakawa (unpublished).

[42] See Supplemental Material at http://link.aps.org/supplemental/10.1103/PhysRevLett.113.143604, which includes Ref. [43], for details of methods and calculations.

[43] G. Nienhuis, Phys. Rev. A **47**, 510 (1993).